Temperature Measurements in a Free Burning Arc

The temperature of a 100 amp GTA welding arc with a 2 mm arc gap is 11,000 K near the cathode and approximately 8,000 K toward the anode

BY S. S. GLICKSTEIN

Introduction

The electric arc has been used with much success in welding for many decades. Nevertheless a comprehensive understanding of the physical phenomena occurring within the various regions of the arc is still lacking. Basically, the arc is a self-sustained gaseous discharge between two electrodes. Its function is to transfer energy to one of the electrodes, i.e., the workpiece. For a given voltage and welding current, the magnitude and distribution of the energy input to the weldment depends to a large extent upon the characteristics of the arc.

Unfortunately, studies of the practical welding arc have been limited, and these have been concerned mainly with a cooled anode (workpiece). The presence of metal vapors introduced into the weld gas from a molten anode can significantly modify the thermal and electrical properties of the gas and affect the behavior of the arc. For example, the ionization potential (IP) of argon is 15.7 eV. By adding significant amounts of low ionization elements such as NI (IP=7.6 eV) the effective temperature of the arc is reduced (Ref. 1). Helium with an ionization potential of 24.5 eV requires a higher discharge voltage and a higher temperature to maintain a stable arc. Since the thermal and electrical properties of the gas are very strongly temperature-dependent as seen in Figs. 1 and 2 (Ref. 2), the characteristics of the arc are significantly different in each case.

S. S. GLICKSTEIN is with the Bettis Atomic Power Laboratory of the Westinghouse Electric Corporation, West Mifflin, Pennsylvania.

Early Investigations

Early investigators, who studied the welding arc, used a cooled anode to prevent its melting and limit the introduction of metal vapor into the arc. Typically, through spectroscopic studies of argon arcs, atomic argon (Ar I), singly (Ar II) and sometimes doubly ionized argon (Ar II) lines have been observed. Investigators (Ref. 3) studying the spectrum of radiation emitted in an argon discharge have reported observing W and La lines emitted from a lanthanated-tungsten electrode (cathode) in addition to Ar I and Ar II lines. Spectral lines from Mn, Fe, Cr, and Al have also been observed from spectroscopic studies of the arc during weldability studies on high manganese stainless steels (Ref. 4). Experiments concerned with vapor emission from molten anodes have been performed in order to extract information on the anode temperature and vapor pressure at the anode (Ref. 5).

Scope of Paper

No studies known to the author have been performed to precisely determine the influence of the molten anode on the behavior of the arc. Therefore, an experimental study of the GTA welding arc was initiated at the Bettis Emission Spectroscopy Laboratory to:

1. Determine the characteristics of the welding arc encountered in "typical" welding conditions at our laboratory.
2. Determine the extent to which vapor emission from a molten anode contributes to the characteristics of the arc configuration and ultimately to the melting of the workpiece.

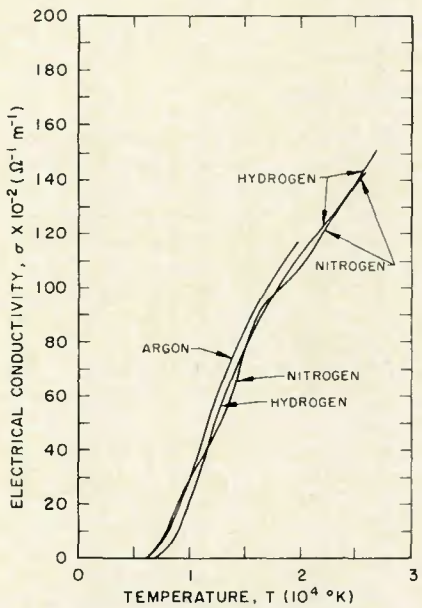

Fig. 1 — Electrical conductivities of argon, nitrogen and hydrogen as a function of temperature (Ref. 9)

This paper presents the results of the initial phase of this program, the purpose of which was to:

1. Set up an experimental arrangement suitable for the study.
2. Develop the experimental technique and analytical procedures for analyzing the data.
3. Determine arc temperatures for different welding conditions.

The paper describes the apparatus employed in the measurements. The

calculational technique for determining the temperature of the arc is outlined, and measured results are presented for various welding arcs. A simplified one dimensional model of the arc is described to explain the observed increase in the diameter of the discharge with increased current. Conclusions are discussed, areas of additional investigations that need to be pursued in the future are outlined.

Apparatus

The spectroscopic analysis of the gas tungsten-arc (GTA) welding arc was performed in the Bettis Emission Spectroscopy Laboratory. A Jarrel Ash flat grating spectrograph with a Wadsworth mounting and a 3.4 meter focal length was used to analyze the spectra emitted from the arc. Kodak Spectrum Analysis Plates No. 3 (SA-3) recorded the spectral lines at a linear dispersion of 0.258 μm/m in the second order. The power supply employed to maintain the discharge was a Vickers Weld Programmer DC Arc Welder 300 amp supply. Argon (99.99%) with a flow rate of 0.0118 m^3/s (15 cfh) was used as the shielding gas for the arc discharge which was maintained in an air environment at atmospheric room pressure.

A gas lens was used with electrodes that were precision ground 2.38 mm (3/32 in.) diameter, 2% thoriated tungsten and had a tip with a 28 ± 4 deg. included angle and a 0.455 mm (0.018 in.) ± 0.076 mm (0.003 in.) flat edge at the tip. They extended 4.75 mm (3/16 in.) from the surface of the No. 5 nozzle.

The arc was focused with lens L_1 to produce a magnified (4.2X) image of the arc at the slits of the spectrograph — Fig. 3. Mirrors M_1 and M_2 were arranged such as to produce a 90 deg. rotation. This was necessary in order to analyze a section of the arc perpendicular to the axis while maintaining the arc axis in a fixed vertical position between the anode and cathode. The image of the arc was moved across the 20 μm slit of the spectrograph by changing the position of the reflecting mirror M_1 which rode on a carrier that was mounted on an optical bar. The total exposure of the recording plate was limited by a rotating sector R which blocked out 90% of the transmitted light, and by the total time the plate was exposed. Typical run times ranged between 20 and 300 seconds.

A standard developing procedure was used for developing all the plates. Four exposures were recorded on the 10 cm x 25.4 cm (4 in. x 10 in.) glass plate. Two plates were used per exposure to span the wavelength region normally set to record from 370 nm to 490 nm. Typical line spectra are shown in Figs. 4 and 5. The intensities of selected lines were scanned from the top to bottom of the lines in 0.5 mm steps using a National Spectrographic Laboratory Microphotometer. Only the peak intensity of the line at each height was recorded.

Although this method simplified the analysis by avoiding integration of the light intensity at each height, it may have introduced much of the experimental uncertainty which was determined later. The relative intensity calibration of the SA-3 plates had been previously determined by personnel at the Emission Spectrographic Laboratory using a standard logarithmic step process (Ref. 6). The corrected relative line intensity I, as a function of measured transmission of light T was fitted to a high order polynomial of the following form:

$$I = \exp (B_0 + B_1 T + B_2 T^2 + \ldots B_8 T^8)$$

where $B_0 = 3.82100$; $B_1 = -0.5346$; $B_2 = 0.03933$; $B_3 = -0.00177$; $B_4 = 0.4818 \times 10^{-4}$; $B_5 = -0.7983 \times 10^{-6}$; $B_6 = 0.7837 \times 10^{-8}$; $B_7 = 0.417 \times 10^{-10}$; $B_8 = 0.9257 \times 10^{-13}$.

The peak intensity distribution from the top to the bottom of the line represents the light emission from a disc — Fig. 6. It was fitted using normalized Chebychev polynomials before undergoing the standard Abel transformation. The Abel transformation was necessary to extract the intensity distribution as a radially dependent quantity. The fitting routine and Abel transformation computer program obtained from Prof. C. Hwang of the University of Pittsburgh were modified to ease the handling of the input and output data.

The absolute intensity of the spectral line was not calculated because of the lack of a standard calibration source needed for this purpose. Due to the rapid decrease of the SA-3 plate sensitivity above 450 nm (Ref. 7), lines above this region were not used although they were very intense and located in a low background region clearly isolated from other

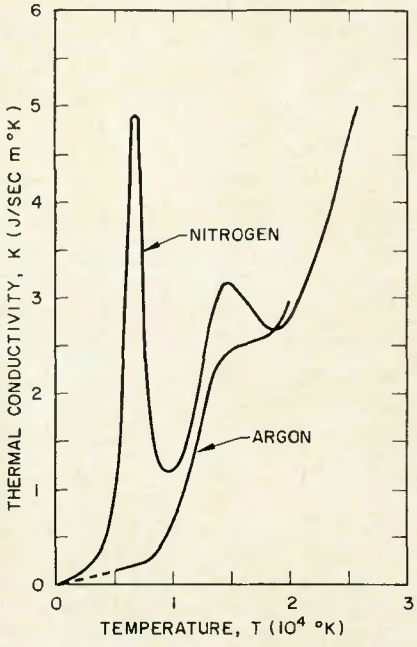

Fig. 2 — Thermal conductivities of argon and nitrogen as a function of temperature (Ref. 9). Pressure = 101 325 Pa (1 atm)

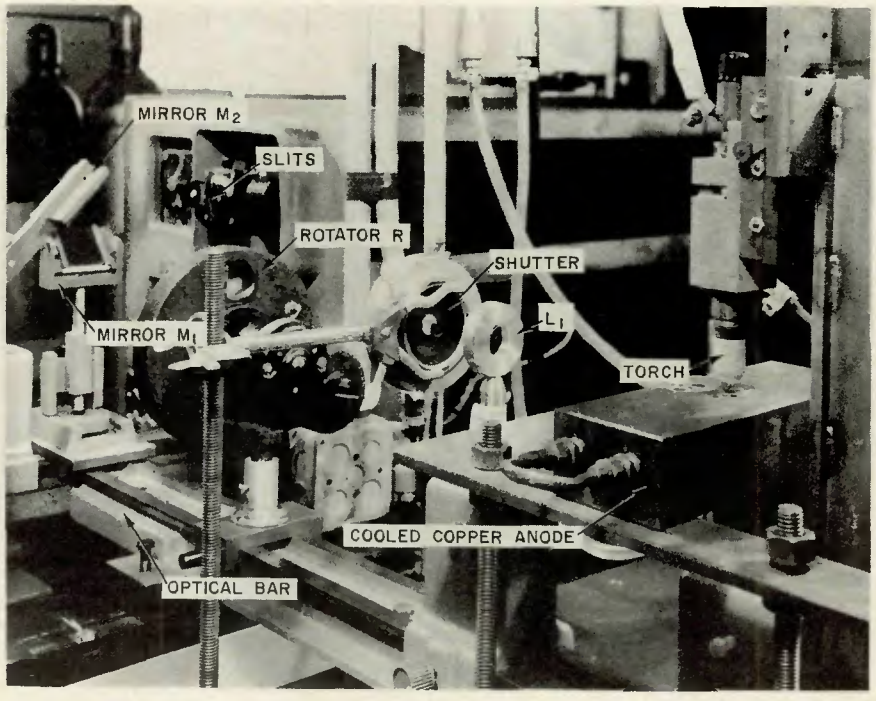

Fig. 3 — Experimental arrangement for spectrographic study of the welding arc

lines. Below 450 nm, the plate sensitivity was assumed constant and may also have contributed to some of the variations in the data points which are noted in the results section of this report.

Determination of Arc Temperatures

The temperature of the arc in a non-equilibrium state can be characterized by various definitions, each leading to different absolute values (Ref. 1). As an example:

1. The "Electron Temperature" is determined by the kinetic energy of the electrons.
2. The "Gas Temperature" is defined by the kinetic energy of the neutral atoms.
3. The "Excitation Temperature" describes the population of various energy levels.
4. The "Ionization Temperature" governs the ionization equilibria.

In the arc column numerous investigators have demonstrated that conditions for only partial thermal equilibrium exists. For the gaseous system to be in complete thermal equilibrium, the following criteria must be met:

1. The velocity distribution of all kinds of free particles (molecules, atoms, ions and electrons) in all energy levels satisfies Maxwell's equation.
2. For each separate kind of particle, the relative population of energy levels conforms to Boltzman's distribution law.
3. Ionization of atoms, molecules, and radicals is described with Saha's equation and dissociation of molecules and radicals with the general equation for chemical equilibrium.
4. Radiation density is consistent with Planck's law.

In the welding arc, there are slight deviations from these conditions. Equilibrium between light quanta and material particles does not exist, resulting in small (few percent) deviation of the radiation from Planck's law (Ref. 1). In addition, in the arc column there exists a radial decrease in tem-

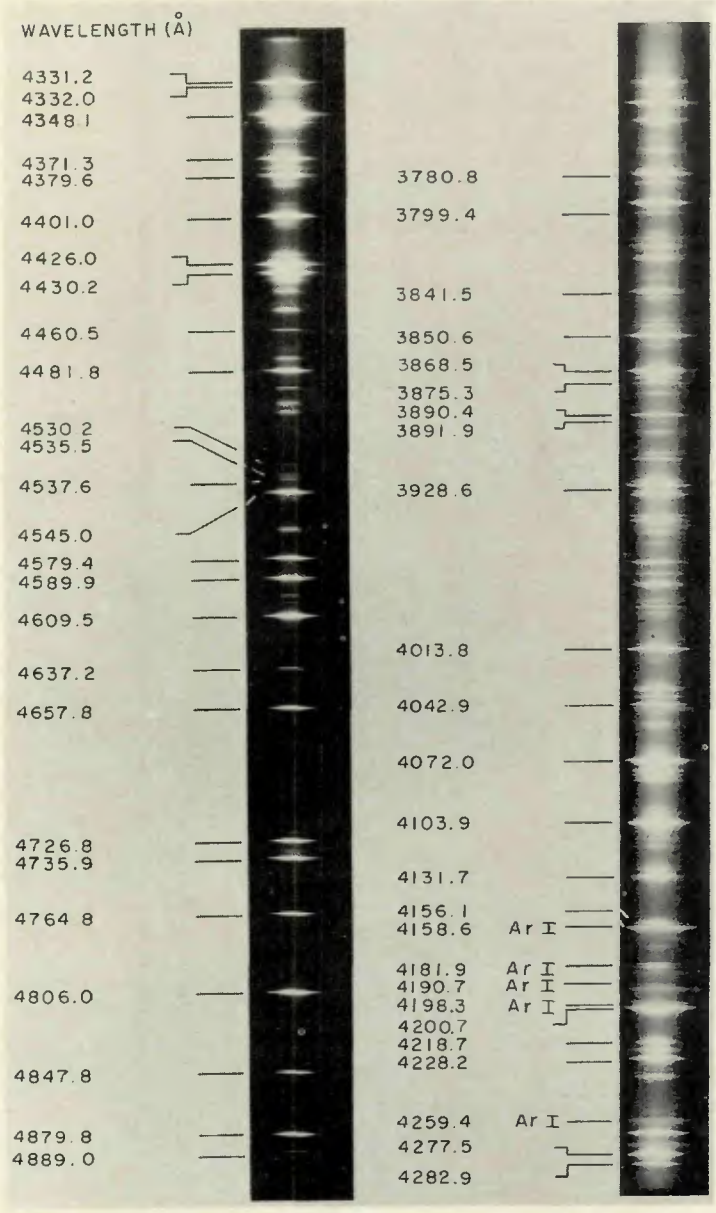

Fig. 4 — Spectrum of 100 amp argon arc between 3700 and 4900 angstroms. The noted wave lengths indicate known lines from ionized argon. Lines denoted by Ar I are from atomic argon

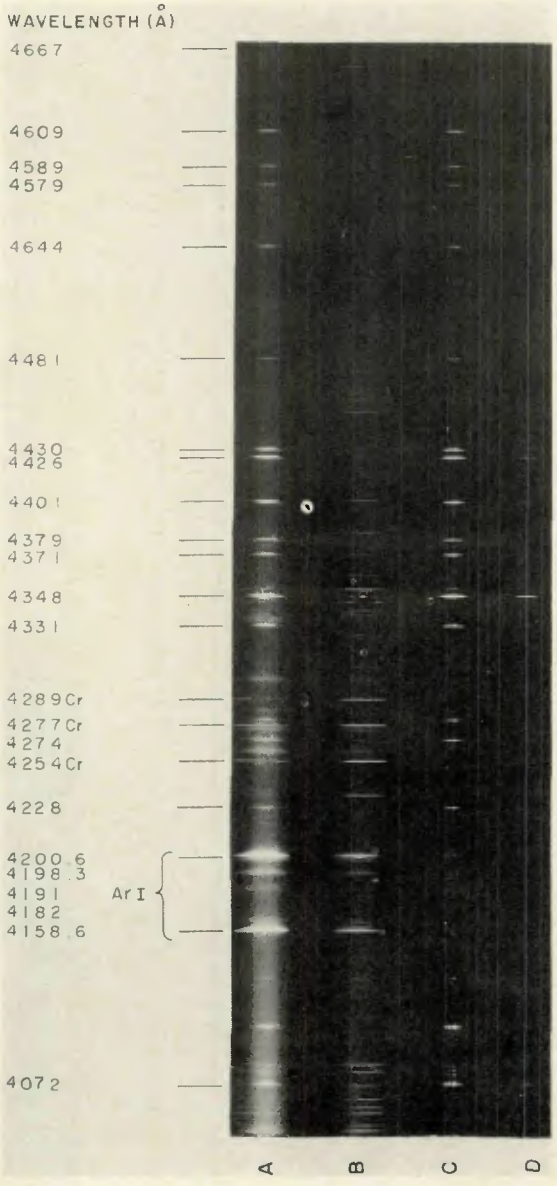

Fig. 5 — Spectral lines from a 100 amp argon arc with an arc gap of 2.0 mm. The length of the line corresponds to a section of the arc perpendicular to the arc axis. Positions A, B, C, D correspond to planes approximately 1.8, 1.5, 1.2 and 0.9 mm from the tip of electrode. The wave lengths of the lines are indicated for some of the Ni, Cr, Ar II, and Mn lines

perature, but the decrease in only one mean free path is small compared to the mean temperature. Thus, it has become customary to consider each element of volume separately and denote the equilibrium conditions in this non-homogeneous source as Local Thermal Equilibrium (LTE).

Under the conditions of LTE, the arc temperature is calculated from the results of intensity measurements of the spectral lines. The intensity I_{qp} of a spectral line emitted by a plasma can be expressed as

$$I_{qp} = \frac{1}{4\pi} A_{qp} \frac{hc}{\lambda_{qp}} N_q \quad (Jm^{-3}\ sr^{-1}\ s^{-1}) \qquad (1)$$

where A_{qp} = transition probability of the atom (or ion) in decaying from level $q \rightarrow p$ (s^{-1}); N_q = concentration or density of excited neutral atoms (or ions) in the level q (number/m^3); c = speed of light (m/s); h = Planck's constant (J s); λ_{qp} = wavelength of the spectral line emitted in the transition $q \rightarrow p$ (m).

If the gas in the discharge is in thermal equilibrium, the population of energy levels for each separate kind of particle follows a Boltzmann distribution, namely,

$$N_q/N_o = (G_q/G_o)\ \exp(E_q/kT) \qquad (2)$$

where N_q = density of particles in excited state q; N_o = density of ground state atoms (or ions); G_q, G_o = statistical weights of the corresponding levels; E_q = excitation energy of the state q; k = Boltzmann constant; T = absolute temperature.

Equations (1) and (2) can be rewritten in the form:

$$\ln(I\lambda/GA) = \ln C_1 - (11600E/T) \qquad (3)$$

Thus,

$$T = -11600E/(\ln(I\lambda/GA) - C_2) \qquad (4)$$

where T is in degrees K and E in electron volts.

The value of T is most readily obtained from the slope of the $\ln(I\lambda/GA)$ vs. E plot for the various spectral lines. (Note: For C_1 to be constant only lines from singly charged ions, or only atom lines must be used.) This technique avoids the necessity of an absolute calibration of the line intensity. The values for the transition probability A, statistical weight G, and excitation energy of the state q from which wavelength λ_{qp} is emitted were taken from the work by Tidwell (Ref. 8) and indicated in Table 1. While recent data have indicated minor variations from these values, within the experimental uncertainty of this experiment the difference did not significantly change the results and the data of Tidwell (Ref. 8) were used throughout.

The above analysis assumed LTE. Numerous investigators have discussed the validity of this assumption and have concluded that in the central region of a typical 100 amp arc this assumption is reasonable. Unfortunately, in the region close to the anode which is extremely important in determining the energy input to the weld surface, conditions for LTE may not be present, and additional experimentation is necessary to determine the effects of non-LTE on the arc temperature in this region. In addition, the experiment was performed with an argon arc in an air environment. The effect of the surrounding air on the argon arc is also uncertain.

Because the line intensity decreases rapidly with temperature (approximately a factor 10 per 500 K), it was difficult to map the entire radial distribution of the arc temperature with a single exposure of the

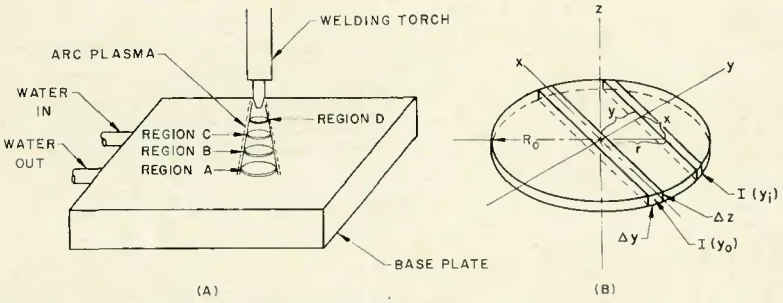

Fig. 6 — Light emission from a disc. (A) welding arc discharge on cooled copper base plate; (B) cross section through the arc plasma showing orientation of a volume element

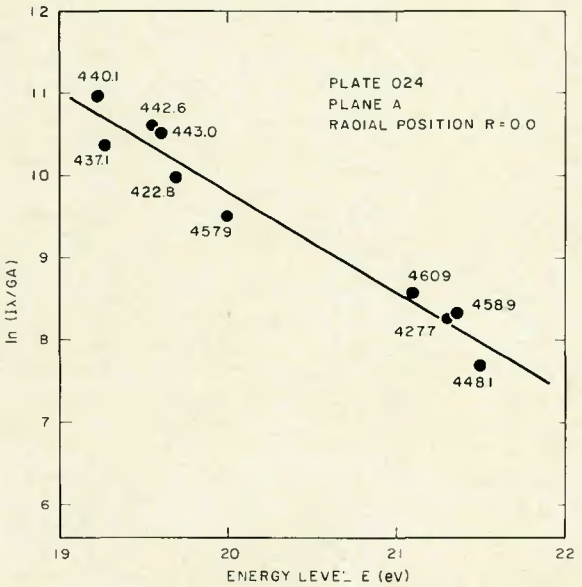

Fig. 7 — Typical plot of ln ($I\lambda$ /GA) vs. energy level E. The temperature of the arc is given by the reciprocal of the slope of the line

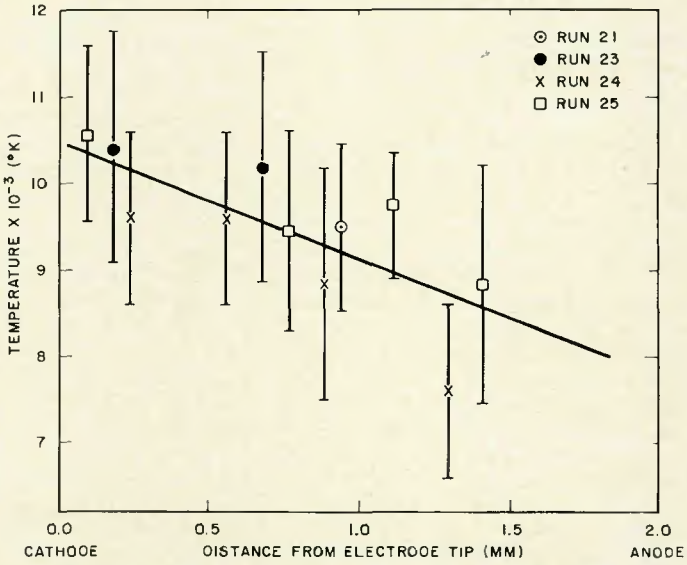

Fig. 8 — Temperature distribution along the axis (R = 0.0) of a 100 amp argon arc. A 2 mm arc gap and a cooled copper anode were used

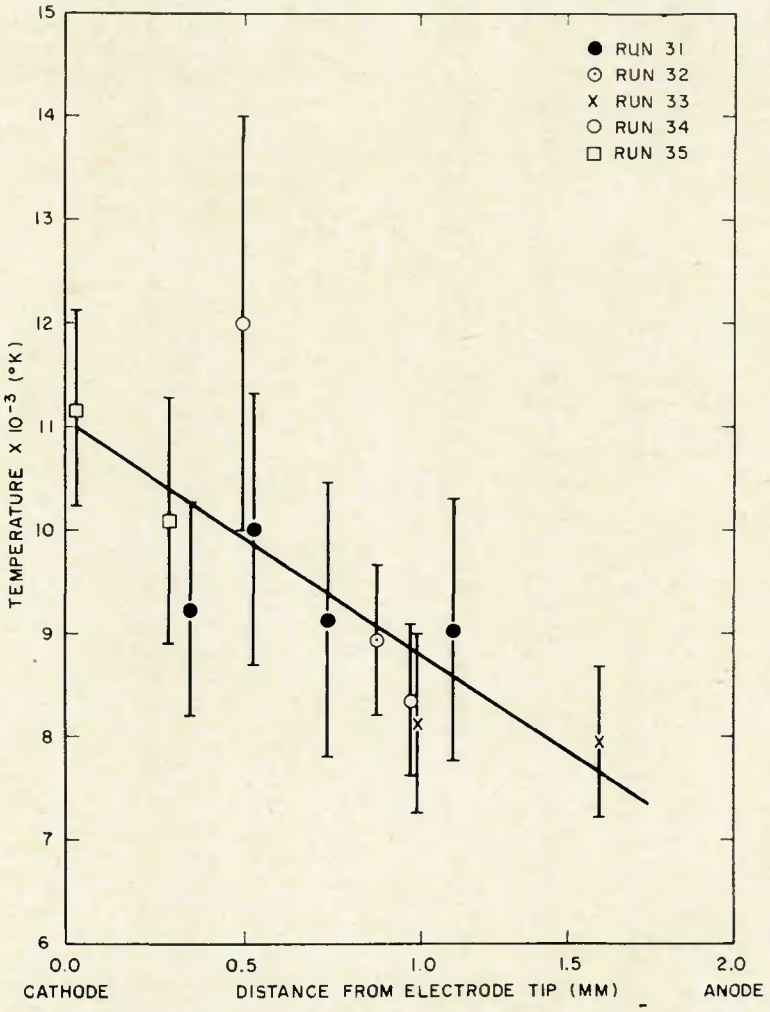

Fig. 9 — Temperature distribution between the anode and cathode at R = 0.010 mm for a 100 amp argon arc with a 2 mm arc gap. The anode consisted of a heated alloy 600 plate

photographic plate since the plates are limited to detecting only an order of magnitude difference in intensity. Thus, measurements were limited to the vicinity of the arc axis only.

Results of Spectral and Photographic Studies

Arc Spectra

The results of a typical argon spectrum taken for a 100 amp welding arc with a water cooled anode are shown in Fig. 4. The observed spectra consist predominantly of lines emitted from excited argon ions and are identified by the notation Ar II. Argon lines emitted from excited atoms are noted by Ar I and are not as frequent in this wave length region.

The spectral lines shown in Fig. 5 were emitted from an Alloy 600 (Ni-Cr-Fe) anode that was not cooled and thus allowed to emit metal vapor into the arc. Compared to the lines emitted from Mn, Ni, and Cr, the argon spectral lines are considerably wider; this is believed to be a result of Stark broadening (Ref. 9).

Axial Arc Temperature Distribution for a Cooled Copper Anode

A typical plot of the $\ln(I\lambda/GA)$ vs. E for different spectral lines is shown in Fig. 7. Measurements of spectral lines emitted from higher energy levels not shown, would improve the straight line fit significantly and greatly reduce the temperature uncertainty. But the spectral lines above 460 nm were not included because of the lack of knowledge of the plate sensitivity vs. wavelength in this region. A least squares fit to the measured data was made to determine the temperature at a point in the arc.

These results are shown in Figure 8 for the 100 amp GTA welding arc with a 2 mm arc gap and a water cooled copper anode. The measured temperatures range from 11000 K near the cathode region to 8000 K at the anode. Very similar results were obtained for points off the axis at R = 0.005 and 0.010 mm.

This is consistent with results published by Gick (Ref. 10) using an electrostatic probe technique to determine the arc temperature of a 100 amp GTA welding arc. In Gick's experiment an arc length of 8 mm was used compared to the 2 mm gap in this study. Additional study is needed to determine precisely the sensitivity of the arc temperature with arc gap.

Table 1 — Spectroscopic Data Used in the Determination of the Arc Temperature (Ref. 8)

Wave length, λ (nm)	Statistical weight, G	Transition probability, A x 10^{-7} (s^{-1})	Energy level, E_q (eV)
484.78	2	8.33	19.3
480.6	6	8.54	19.22
476.48	4	4.86	19.87
473.5	4	6.30	19.26
472.6	4	7.23	19.76
465.78	4	6.77	19.8
460.95	8	12.32	21.1
458.99	6	9.92	21.3
457.9	2	6.97	19.97
448.1	6	13.34	21.5
443.0	4	5.33	19.61
442.6	6	6.70	19.55
440.1	6	3.17	19.22
437.1	4	2.48	19.26
435.2	2	2.01	19.3
434.8	8	13.52	19.49
427.7	4	9.58	21.35
422.8	6	1.83	19.68

Axial Arc Temperature Distribution for a Heated Anode

Spectral measurements were made with a heated anode using Alloy 600 plates 5.08 cm × 5.08 cm × 0.625 cm thick. A molten weld puddle was allowed to form, and after waiting approximately 60 seconds for some form of equilibrium condition to be reached, the spectrum of the arc was measured. Unfortunately, during the data accumulation time some crud formed around the perimeter of the pool which partially obscured the arc near the anode surface. In addition crystals in the form of whiskers sometimes appeared on the cathode.

If long exposures were attempted, melt-through would occasionally occur causing the puddle to sink. It was therefore difficult to maintain an equilibrium condition. This could readily explain why there was significantly more scatter in the experimental data for the molten anode. Nevertheless, we arrive at an approximate indication of the arc temperature which is comparable to what was obtained for the cooled anode as shown in Fig. 9.

DeGalan (Ref. 11) in his study on dc carbon arcs, indicated arc temperatures for metal vapor arcs on the order of 4000 K. This is definitely not the case for the type of arcs produced during welding with Alloy

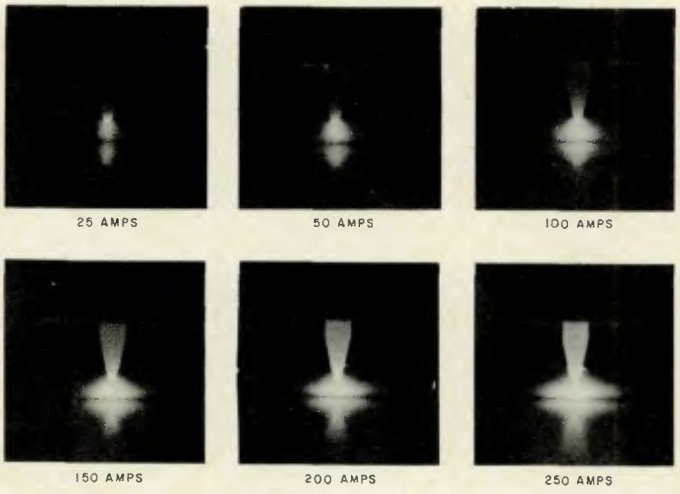

Fig. 10 — Photographs of an argon arc taken with Type 58 Polaroid film and a No. 25 filter for various weld currents. The arc gap was 2.0 mm. The cathode consisted of a 2.35 mm thoriated tungsten electrode and a water-cooled copper anode

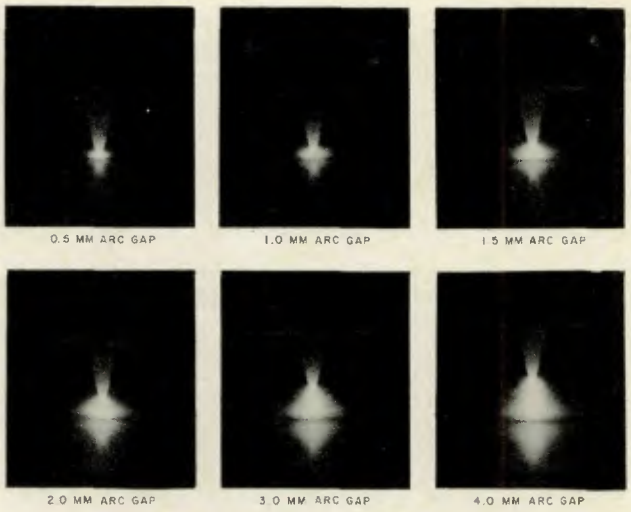

Fig. 11 — Photographs of an argon arc taken with a Type 58 Polaroid film and a No. 25 filter for various gap spacings. The welding current was 100 amp. The cathode consisted of a 2.35 mm thoriated tungsten electrode and a water-cooled copper anode

600. While the vapors of Ni, Cr, and Mn were very clearly present in the arc, the amount was not sufficient to cause a factor of two reduction in the arc temperature. In addition photographs of the arc taken with a molten anode revealed no noticeable difference compared to the cold anode.

It is concluded, within the experimental uncertainty, the temperature along the arc axis is approximately the same for the cooled anode and molten anode experiments. But the uncertainty is large and, within this temperature uncertainty, significant changes in electron density and thus electrical conductivity may exist.

Photographic Analysis of the GTA Welding Arc

The magnitudes of temperatures measured along the arc axis are significantly below the results reported by Olsen (Ref. 12) using higher arc currents. The temperature near the cathode reported by Olsen for a 400 amp arc was near 22000 K and decreased near the cathode to 16000 K. Olsen reported that the plasma had a tendency to spread with increased current rather than raise its maximum temperature above 22,000 deg. K. He attributed this to the fact that the electrical conductivity passed through a maximum at that temperature and rather than increase the temperature with little or no change in electrical conductivity, the plasma appeared to expand.

This reasoning is not justified in the case of the low current arcs found in this study because the temperature range established by the present measurements is on the order of 10,000 K. As indicated in Figs. 1 and 2 the electrical and thermal conductivity changes rapidly in this temperature region. Nevertheless, the arc plasma does expand with increased current as is concluded from photographs of the arc taken with polaroid film (type 58) employing a number 25 filter.

The results are shown in Fig. 10 for a current range between 25 and 250 amp. Clearly visible is the inner core of the arc not normally visible without suitable filtering. In addition Figure 11 also shows the results of arc configuration changes that occur when the arc gap spacing is varied from 0.5 mm to 4.0 mm. While the absolute magnitude of the arc width was found to be logarithmically dependent upon the exposure, and also upon the type of filter used, the trend observed in Figs. 10 and 11 for constant exposure and filter are significant.

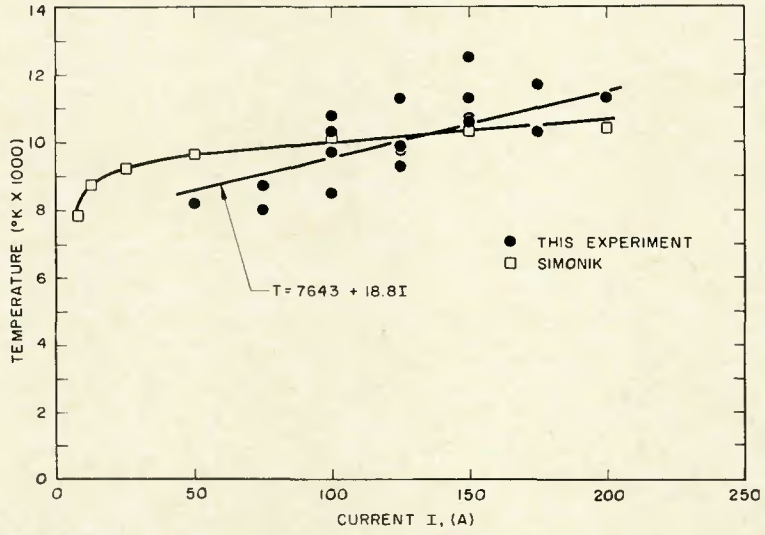

Fig. 12 — Dependence of arc temperature on arc current. The temperatures in this experiment were measured on the axis of the mid-plane of a GTA welding arc, 2 mm arc gap

Dependence of the Arc Temperature on Arc Current

To determine the sensitivity of the arc temperature T, to variations in the arc current I, spectral measurements were made at the mid-plane of an arc for a 2 mm arc gap, using a cooled copper anode. The results are shown in Fig. 12 for the current range between 50 to 200 amp. The uncertainty in each of the measurements ranged from 10-30%. A least square fit to the data assuming a linear dependence of the form

$$T = T_o + mI \qquad (5)$$

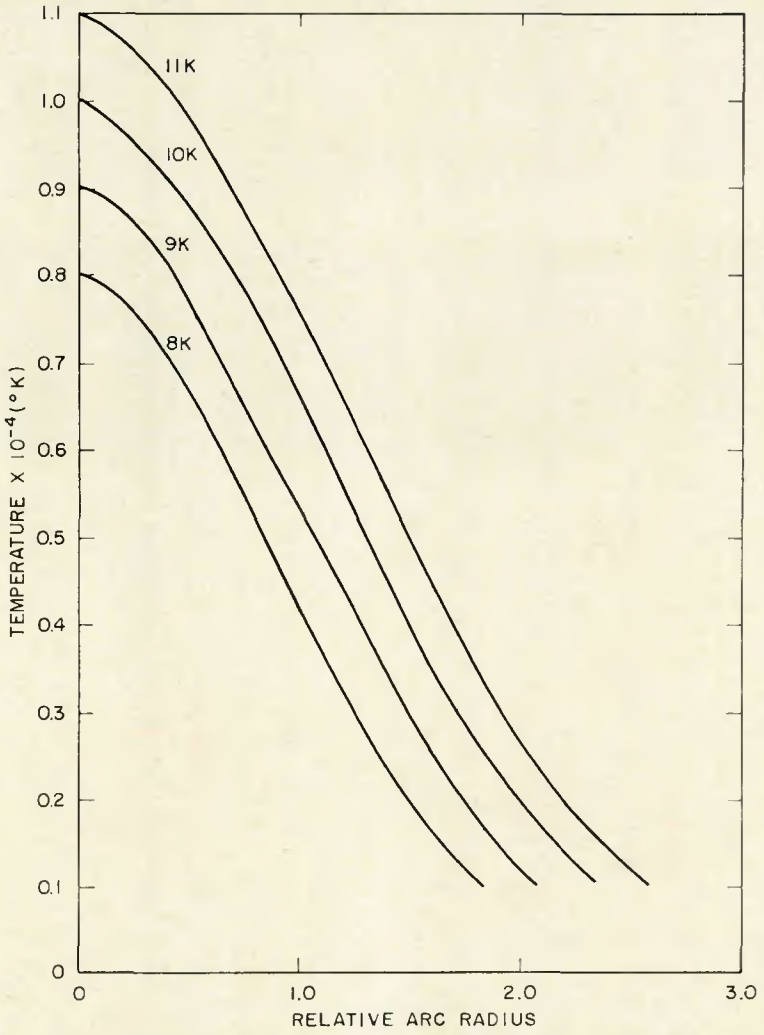

Fig. 13 — Calculated radial distribution of temperature for different peak temperatures on the axis

implies T_o = 7643 ± 559 K and m = 18.8 ± 2.8 K A.

The only other measurement known to the writer in this current range for an argon arc is shown in Fig. 12, but this employed carbon electrodes (Ref. 13). Comparisons to other measurements are difficult because the electrode material and electrode shape in a welding arc will influence the arc configuration and temperature distribution. The change in arc configuration with electrode shape has previously been discussed in the literature (Ref. 14, 15).

The measured increase in arc temperature with increased arc current can readily explain the observed expansion of the plasma region seen in Fig. 10. This is discussed below where a simplified one dimensional arc is analyzed.

One Dimensional Arc Model

In order to explain the radial expansion of the plasma region with increased arc current a simplified model of the arc in one dimension is considered. This is described in the literature, as a "channel model" (Ref. 16). For arcs that are bounded radially as in a tube enclosure or for arcs with large arc gaps such that the energy flow in the axial direction at the center of the arc may be considered as negligible, the channel model is readily applicable.

For the welding arc with a short arc gap as has been discussed in this study, axial energy transfer must be considered in any detailed analysis. Nevertheless, the simple picture described in the channel model will provide the necessary insight to explain the plasma expansion.

The model is based on a balance between the heat generation by Joule effect and heat transfer by thermal conductivity. The equation describing this is known as the Elenbaas-Heller equation and for one dimensional heat flow may be written as:

$$\sigma E^2 = -(1/r)\,(d/dr)\,(rK(dT/dr)) \quad (6)$$

where σ = electric conductivity; K = thermal conductivity; E = uniform electric field; T = temperature.

The solution of eq (6) is not as simple as it looks because σ and K depend upon the plasma temperature. Nevertheless in order to get an analytical solution we shall assume $\sigma = \sigma_o T^2$ and $K = K_o T$. By substituting these values for σ and K in eq (6) and applying the boundary condition at r = 0, T(0) = T_m

$$T(r) = [T_m^2 J_o (2\sigma_o E^2 r^2/K_o)]^{1/2} \quad (7)$$

where J_o is a Bessel function of zeroth order.

Thus, increasing the peak temperature T_m at r = 0, which has been shown experimentally to result from an increase in weld current, will produce a direct increase in the radial temperature. This is observed as an expansion of the visual plasma region.

More realistically, Hoyaux (Ref. 16) shows that $\sigma = \sigma_o T^{3/2}$ and $K = K_o T^{5/2}$. With this functional dependence of σ and K, the Elenbaas-Heller equation can no longer be solved analytically. Nevertheless numerical solutions can be found (Ref. 16) and results shown in Fig. 13 yield the same conclusions as discussed above.

Conclusions

The results of measurement of a 100 amp argon GTA welding arc with an arc gap spacing of 2 mm indicate an arc temperature near the cathode of 11000 K which decreases toward the anode to ~ 8000 K. At this temperature the fraction of argon gas ionized varies from 0.2 to 6%. The electron density and electrical conductivity of the gas is very sensitive to small changes in the arc temperature in this temperature range.

The arc temperature results determined with a stationary molten anode are similar to the results with a cooled anode. This is surprising since the low ionization material such a Ni, Cr, and Mn seen in the spectrum was expected to produce a considerably lower arc temperature. Photographs of the arc indicate an expanding plasma region with increased arc current; this is explained by the increase in the peak temperature on the axis as the current is raised. The dependence of the axial temperature at the midplane of the arc was determined, and may be approximated by T = 7643 + 18.8 I K.

Further study is needed to investigate the welding arc under more refined experimental conditions. This must include suitable control of the environment surrounding the arc. The electrode configuration and arc gap spacing have been shown to in-

fluence the arc configuration. Additional effort is needed to determine how the arc temperature is influenced by these parameters. Since this paper was written, Mechev and Eroshenko reported the results of such studies (Ref. 17). The existence of local thermodynamic equilibrium conditions needs to be further investigated, especially for regions close to the anode. Equilibrium must be established for the molten anode experiments.

Chase (Ref. 17) has shown that minor elements in the base material can affect arc voltage. This should be reflected in changes in the magnitude and distribution of the arc temperature. While recent analytical studies of the anode region have been reported (Ref. 2, 19), additional analytical and experimental studies are needed in regions close to the anode surface in order to better understand the contraction mechanism that occurs in this region. Its effect on the energy input distribution to the anode surface is a vital factor ultimately influencing weld penetration.

Acknowledgment

I would like to express my appreciation to Dr. W. Yeniscavich who introduced me to the problems in welding and offered continuous encouragement throughout this study. I also wish to acknowledge the support provided by members of the Bettis Emission Spectroscopy Laboratory in helping to set up the experiment and to Prof. C. Hwang for supplying the computer routine for performing the Abel transformation.

References

1. Bowman, P. W. J. M., *Theory of Spectrochemical Excitation*, Plenum Press N.Y., 1966.

2. Chou, T. S., "Anode Contraction Mechanism of High Intensity Arcs," Ph.D. Dissertation, Univ. of Minn., 1971.

3. Mechev, V. S., and Eroshenko, L. E., "Determining the Temperature of the Plasma in an Arc Discharge in Argon," *Avt. Svarka, 8*, 1970.

4. Bennett, W. S., and Mills, G. S., "GTA Weldability Studies on High Manganese Stainless Steels," *Welding Journal*, Vol. 53 (12), Dec. 1974, Res. Suppl., pp. 548-s to 553-s.

5. Howden, D. G., "Mass Transfer of Metal Vapor and Anode Temperature in Arc Melting," *Welding Journal*, Vol. 48 (3), March 1969, Res. Suppl., pp. 125-s to 132-s.

6. "Methods for Emission Spectrochemical Analysis," ASTM 6th Edition, p. 74, 1971.

7. Kodak, "Materials for Emission Spectrography," 2nd Edition, 1968.

8. Tidwell, E. D., "Transition Probabilities of Argon II," *J. Quant. Spectrosc. Rad., 12*, 431 (1972).

9. Shaw, Jr., C. B., "Diagnostic Studies of the GTAW Arc," *Welding Journal*, Vol. 54 (3), Feb. 1975, Research Suppl., pp. 81-s to 86-s.

10. Gick, A. E. F., Quigley, M. B. C., and Richards, P. H., "The Use of Electrostatic Probes to Measure the Temperature Profiles of Welding Arcs," *J. Phys. D. Appl. Phys. 6*, 1941-9 (1973).

11. DeGalan, L., "Particle Distribution in the D.C. Carbon Arc," Ph.D. Dissertation, Druk: V. R. B. Kleine der A3-4 Groninger, 1965.

12. Olsen, H. N., "Determination of Properties of an Optically Thin Argon Plasma" in *Temperature*, Vol III, Reinhold Pub. Co. N.Y. Part 1, 1962.

13. Simonik, A. G., and Pongil'skaya, L. N., "Approximation of the Temperature of the Arc Current in Terms of the Effective Ionization Potential and the Welding Current," *Svar. Proiz.*, 2, 1974.

14. Glickstein, S. S., Friedman, E., and Yeniscavich, W., "Investigation of Alloy 600 Welding Parameters," *Welding Journal*, Vol. 54 (4), Apr. 1975, Research Suppl., pp. 113-s to 122-s.

15. Spiller, K. R., and MacGregor, G., "Effects of Electrode Vertex Angle on Fused Weld Geometry in TIG Welding," in "Proc. of the Conf. on Advances in Weld Processes, April 1970," The Weld Inst., Abington Hall, Cambridge, 1971.

16. Hoyaux, M. F., "Arc Physics," Springer-Verlag N.Y., 1968.

17. Mechev, V. S., and Eroshenko, L. D., "The Axial Distribution of Temperature of an Electric Arc Burning in Argon," *Art. Svarka*, 6, 14-17 (1975).

18. Chase, Jr., T. F., "The Effect of Anode Composition on Tungsten Arc Characteristics," Ph.D. Dissertation, Rensselaer Polytechnic Institute, 1970.

19. Chou, T. S., and Pfender, E., "Spot Formation at the Anode of High Intensity Arcs," *Warme und Stoff. 6*, (1973).